DOE/ER/61202-1

Steady-State and Transient Modeling of Tracer and Nutrient Distributions in the Global Ocean

DOE/ER/61202--1

DE92 011805

Progress Report

for Period June 1, 1991 - March 31, 1992

Thomas F. Stocker & Wallace S. Broecker

Lamont-Doherty Geological Observatory of Columbia University

Palisades, New York, 10964

March 26, 1992

Prepared for

The U.S. Department of Energy

Agreement No. DE-FG02-91ER61202

DISCLAIMER

Abstract

The deep circulation model of Wright & Stocker (1992) has been used to represent the latitude-depth distributions of temperature, salinity, radiocarbon and "color" tracers in the Pacific, Atlantic and Indian Oceans. Restoring temperature and salinity to observed surface data the model shows a global thermohaline circulation where deep water is formed in the North Atlantic and in the Southern Ocean. A parameter study reveals that the high-latitude surface salinity determines the composition of deep water and its flow in the global ocean. Increasing Southern Ocean surface salinity by 0.4 ppt the circulation changes from a present-day mode where North Atlantic Deep Water is important to one where Antarctic Bottom Water is dominant.

An inorganic carbon cycle with surface carbonate chemistry is included, and gas exchange is parameterized in terms of pCO_2 differences. Pre-industrial conditions are achieved by adjusting the basin-mean alkalinity. A classical $2\times CO_2$ experiment yields the intrinsic time scales for carbon uptake of the ocean; they agree with those obtained from simple box models or 3-dimensional ocean general circulation models. Using the estimated industrial anthropogenic input of CO_2 into the atmosphere the model requires, consistent with other model studies, an additional carbon flux to match the observed increase of atmospheric pCO_2.

We use more realistic surface boundary conditions which reduce sensitivity to freshwater discharges into the ocean. In a glacial-to-interglacial experiment rapid transitions of the deep circulation between two different states occur in conjunction with a severe reduction of the meridional heat flux and sea surface temperature during peak melting. After the melting the conveyor belt circulation restarts.

1 Towards a Realistic Present-Day Deep Circulation

1.1 Model Extension

The deep ocean circulation model of Wright & Stocker (1992) is based on the original formulation of Wright & Stocker (1991) and solves the zonally averaged balance equations of momentum, mass, energy and salt in an ocean basin. The east-west pressure difference, which arises upon zonally averaging the momentum balance is parameterized in terms of the meridional pressure gradient.

This is consistent with results from a 3-dimensional general circulation model. The global model based on zonally averaged equations includes the three major ocean basins of the Pacific, Atlantic and Indian Oceans, and properties are exchanged between them in a circumpolar Southern Ocean. The model has already been used to investigate the global thermohaline circulation, its multiple equilibria and sensitivity to steady meltwater discharges (Stocker & Wright, 1991a,b; Stocker *et al.*, 1992a).

During the first year of this project we have made several extensions to the model. They were necessary to bring the modeled tracer fields into closer agreement with observations. These improvements were done in close collaboration with Dr. Daniel Wright (Bedford Institute of Oceanography) who is a consultant for this project and has spent a month at Lamont-Doherty (12. October to 14. November 1991). We have now included a fully non-linear, pressure-dependent equation of state and modified the convection scheme. An arbitrary number of three types of passive tracers can be modeled: (i) stable tracers, (ii) radioactively decaying tracers and, (iii) ideal age tracers. Another extension which causes a more realistic circulation in the deep ocean is the inclusion of a meridional ridge in the Southern Ocean. This enables the geostrophic northward transport of deep water masses formed around Antarctica. A detailed description of the model modifications and their consequences is found in Wright & Stocker (1992) and Stocker *et al.* (1992b, see Appendix).

1.2 Sensitivity to High-Latitude Forcing

Using the sea surface temperatures (SST) and salinities given by Levitus (1982) the deep water masses in the model are dominated by North Atlantic Deep Water (NADW), and only little Antarctic Bottom Water (AABW) is present in the South Atlantic. We found that the characteristic distribution of radiocarbon observed in GEOSECS is not reproduced. It is well known that the annual mean surface data of temperature and salinity in the highest latitudes are summer biassed and hence underestimate the forcing density at the surface. If the model is driven by the salinities of the observed deep water in the Southern Ocean, AABW forms at a more realistic rate and intrudes far north in the Atlantic, thereby modifying the deep-ocean density structure, and reducing and shallowing NADW formation. We have performed a sensitivity study of the high-

latitude forcing and show that very different tracer fields can be obtained by altering the restoring salinity (Appendix).

If the deep water formed in the Southern Ocean has about the same high-latitude restoring salinity as that formed in the North Atlantic a global circulation results that is broadly consistent with the reconstructions for the Last Glacial Maximum (Boyle & Keigwin, 1987; Duplessy *et al.*, 1989). NADW is replaced by intermediate water formation not exceeding 3000m depth. Below it the water masses are of AABW origin. Using a tracer that distinguishes water mass origins it is shown that in the glacial North Atlantic a strong vertical gradient is present, while the depth-profiles of the modern ocean are almost uniform and dominated by waters of North Atlantic origin.

2 Inorganic Carbon Cycle

We have added to the ocean circulation model an inorganic carbon cycle including borate as in Maier-Reimer & Hasselmann (1987). The chemical equilibria are given by

$$H_2O + CO_2 \rightleftarrows H^+ + HCO_3^- ,$$

$$HCO_3^- \rightleftarrows H^+ + CO_3^= ,$$

$$H_2O \rightleftarrows H^+ + OH^- ,$$

$$H_2OB(OH)_3 \rightleftarrows H^+ + B(OH)_4^- ,$$

with the dissociation constants defined as

$$K_1 = \frac{[H^+][HCO_3^-]}{[CO_2]} ,$$

$$K_2 = \frac{[H^+][CO_3^=]}{[HCO_3^-]} ,$$

$$K_W = [H^+][OH^-] ,$$

$$K_B = \frac{[H^+][B(OH)_4^-]}{[H_2OB(OH)_3]} .$$

These dissociation constants are strong functions of temperature and salinity as well as pressure (Mehrbach *et al.*, 1973; Weiss, 1974). The system can be reduced assuming a total borate concentration of $4.106 \cdot 10^{-4}$mole/kg (at S=35ppt, Culkin, 1965) and by defining two new variables, total carbon, ΣC, and alkalinity, A, according to

$$\Sigma C = [CO_2] + [HCO_3^-] + [CO_3^=] ,$$
$$A = 2[CO_3^=] + [HCO_3^-] + [OH^-] + [B(OH)_4^-] - [H^+] ,$$

which are conserved tracers. In an inorganic model alkalinity is only affected by dilution by freshwater fluxes at the surface of the ocean and can hence be recovered by simple scaling from salinity. We use mean values of A=2373μeq/kg and S=35ppt. For total carbon the full advection diffusion equation is solved:

$$\frac{\partial \Sigma C}{\partial t} + \frac{1}{a \cos\phi} \frac{\partial (\cos\phi v \Sigma C)}{\partial \phi} + \frac{\partial w \Sigma C}{\partial z} = \frac{1}{a^2 \cos\phi} \frac{\partial}{\partial \phi} (\cos\phi K_H \frac{\partial \Sigma C}{\partial \phi}) + \frac{\partial}{\partial z} K_V \frac{\partial \Sigma C}{\partial z} + q_{\Sigma C}^{conv} ,$$

where all quantities are zonal averages, (ϕ, z) are latitude-depth coordinates with z positive upwards, a is the radius of the Earth, (v, w) are the meridional and vertical velocities, K_H and K_V are the horizontal and vertical diffusivities; $q_{\Sigma C}^{conv}$ denotes vertical fluxes due to convection.

No-flux conditions for the tracer are applied at the bottom and the lateral boundaries of the basin, while at the surface we assume that the ocean-to-atmosphere flux of carbon is proportional to the difference in partial pressures, viz.

$$F_{\Sigma C} = \lambda \, (pCO_2|_{\text{ocean}} - pCO_2|_{\text{atmosphere}}) ,$$

where we take a constant gas exchange rate $\lambda = 0.05 \frac{\text{mol}}{\text{m}^2\text{yr ppm}}$. This is the value used by Maier-Reimer & Hasselmann (1987) and reviewed by Sundquist (1985). From the atmospheric inventory of carbon we calculate pCO_2(atm), and pCO_2(ocean) is determined solving the carbonate chemistry

using the dissociation constants that are functions of temperature and salinity (Takahashi *et al.*, 1980). Table 1 gives the global inventory of carbon for a typical pre-industrial state; the values compare well with those estimated by Sundquist (1985).

Figure 1 shows the partial pressure difference $\Delta pCO_2 = pCO_2|_{ocean} - pCO_2|_{atmosphere}$ in the three ocean basins which are roughly consistent with (Maier-Reimer & Hasselmann, 1987). Direct comparison with observation is premature because of the absence of the biological pump.

The present steady state of the inorganic model shows surface-to-bottom contrasts in total carbon of less than about 165μmole/kg, about half of that observed (Takahashi *et al.*, 1981). This is caused by the absence of the biological pump which acts as a downward flux of carbon to enhance the gradient that is already maintained by the solubility pump.

2.1 Double-CO_2 Experiments

In developing a carbon cycle model we have to check its consistency with previous studies, in particular with those that employ dynamical ocean models to calculate the uptake of excess CO_2. A useful comparison consists of determining the time scales involved in the uptake of CO_2 after the atmospheric content has been instantly doubled. The analyses of Sundquist (1985) and Maier-Reimer & Hasselmann (1987) assume that the time dependent airborne fraction, which is defined as

$$a(t) = \frac{1}{r-1}\frac{p(t)-p_0}{p_0} \ ,$$

where $p(t)$ is the atmospheric CO_2 partial pressure at time t, p_0 is the pre-industrial reference and $p(0) = r\,p_0$, can be approximated by a sum of exponentials of the form

$$a(t) = A_0 + \sum_{i=1}^{N} A_i e^{-\frac{t}{\tau_i}} \ .$$

A_0 is the asymptotic airborne fraction and the A_i and τ_i are the amplitudes and time scales of the uptake, respectively; they are characteristic values of the particular model steady state. If the

uptake in the model is a linear process, the atmospheric partial pressure can be calculated for any uptake function once the characteristic values have been determined.

In Tab. 1 the characteristic values of the present steady state are compared to the results of Maier-Reimer & Hasselmann (1987) and Sarmiento *et al.* (1992); again, satisfactory agreement is found. Note that the largest differences from the Hamburg model are found at the shorter time scales indicating that the zonally averaged model at the present steady state will yield different uptake rates for very short term runs. This may be due to the absence of horizontal wind-driven gyre circulation in the present model. Another source of underestimating the uptake on shorter time scales could be in the Southern Ocean where we presently use a course resolution. Using realistic surface boundary conditions for radiocarbon we found that the surface residence time of tracers in the southern high-latitudes is too long (see Appendix). However, this is an area where a detailed parameter study will be necessary. Figure 2a gives $a(t)$ as calculated from Tab. 1 for the present (solid), the Hamburg (1-dashed) and the Princeton (2-dashed) models.

2.2 Industrial Input 1800 – 2000

As a final test of the consistency of the inorganic carbon cycle in this model we have performed a transient experiment using observed data. The model is spun up to steady state for 10,000 years, starting with a mean value $\Sigma C = 2115 \mu$mole/kg. In a few short integrations (2000 years) different mean alkalinities were used to determine the value that yields a pre-industrial atmospheric $pCO_2$of about 281ppm. Siegenthaler & Oeschger (1987) summarize various studies with pre-industrial values in the range of $pCO_2 = 281 \pm 7$ppm. The inventory was presented in Tab. 1. We then took the anthropogenic carbon input rates given by Rotty (1981) and integrated the model forward in time for 180 years. From the deviations of the modelled pCO_2 to the observed an additional source function is reconstructed with the help of a deconvolution using the characteristic values determined above. Figure 2b shows a time series of the anthropogenic input and the source function calculated to match the observed industrial evolution of pCO_2. The present ocean model requires a source of carbon dioxide prior to about 1940 of a maximum of 0.6 Gt/yr after which there is a nearly linear decrease to -0.9 Gt/yr for 1983. This is consistent with Sarmiento *et al.* (1992).

This comparison demonstrates that the present model reproduces results from much more expensive and sophisticated dynamical models *in a quantitative manner*. The present model was especially developed for long-time integration (over many thousands of years) and is capable of reproducing the present climate state including the large scale features of the observed interannual variability. The next step, therefore, is to perform experiments which address the transitions of the deep ocean circulation from a glacial to an interglacial mode and study the implications this has on the carbon cycle.

3 Stability of the Deep Circulation

It has become clear that glacial-to-interglacial climate change is associated with changes of the deep circulation in the world ocean (Broecker & Denton, 1989). Before attempting to model such transitions in a carbon cycle model, physically realistic transitions between different modes of the circulation must be realised and studied. During the last few years ocean circulation models of various complexity have shown multiple equilibria when forced with mixed surface boundary conditions, i.e. heat fluxes are proportional to the deviation of the model's SST from a fixed observed value and freshwater fluxes are held constant (Bryan, 1986; Maier-Reimer & Mikolajewicz, 1989; Marotzke & Willebrand, 1991; Wright & Stocker, 1991; Stocker & Wright, 1991a,b). This solution structure also carries over to fully coupled models (Manabe & Stouffer, 1988; Stocker *et al.*, 1992) where the boundary conditions are supposedly more realistic. However, all these models exhibit a strong sensitivity to salinity and freshwater flux perturbations. Deep water formation in the North Atlantic can be shut off with freshwater flux anomalies as small as 0.01 Sv ($1Sv=10^6 m^3/s$). This seems to be in conflict with the observation that modern NADW formation has been relatively stable over the last 8000 years. Some fundamental stabilizing feedback mechanism must therefore be missed when using this type of boundary condition.

Furthermore, deglaciation experiments with these models have always reproduced a fast destruction of the conveyor belt within a couple of decades but *never* its subsequent resumption after the shutdown. Stocker & Wright (1991a) have shown that NADW can be switched back on if it is

assumed that the hydrological cycle in the atmosphere changes slightly. Although consistent within the model framework, this represents an external forcing mechanism.

Preliminary experiments (in collaboration with Dr. Daniel Wright) using the present model with different types of boundary conditions indicate that more realistic formulations of these conditions will enable the recovery of collapsed circulations during pulse meltwater events. While mixed boundary conditions are reasonable for freshwater fluxes, they have the problem of completely ignoring the thermal feedback to reduced oceanic meridional heat transport on the atmosphere. When SST decreases this can create local temperature anomalies in the atmosphere which mitigate an immediate and local increase of a compensating atmosphere-to-ocean heat flux. One limiting case is the use of *full* flux boundary conditions, i.e. fixing both heat and freshwater fluxes at their steady state values. Another, similar limiting case would be to consider a "zero heat capacity" atmosphere (Zhang *et al.*, 1992).

The meltwater history of Fairbanks (1989) was approximated by an analytic expression and used as the freshwater anomalies discharged at 14°N into the Atlantic; the maximum value is 0.45 Sv. Under mixed boundary conditions this would cause a transition to the second equilibrium with a reversed Atlantic thermohaline circulation. With the full flux or the zero heat capacity boundary conditions the freshwater flux is able to interrupt deep water production for the time of increased melting discharge. Once the melting is over, the circulation recovers, and the conveyor belt resumes operation. The recovery of deep water formation is due to the fact that this type of boundary condition fixes both heat and freshwater flux divergence at the surface and hence defines uniquely the eventual steady state (Welander, 1986).

However, we emphasize that these boundary conditions are not realistic either, although they exhibit reasonable transient behaviour of the circulation. During the shut-off of the northward meridional heat supply into the Atlantic, SST drops as low as −50°C. Hence, an ice model (or some parameterisation of it) must be included if one is to understand the transient behaviour of the ocean during a glacial termination. One step towards this goal is to make the following assumption. When SST falls below the freezing point, an insulating sea ice cover is formed which inhibits surface fluxes of heat and freshwater and holds SST at the freezing temperature. Where no ice is present, full

flux boundary conditions are used.

The total freshwater flux at 14°N (including the steady state flux of −0.1 Sv) is given in Fig. 3a. The evolution of SST at 72°N the maximum overturning streamfunction and the Atlantic meridional heat flux crossing 45°N are shown in Figs. 3b-d. Once a critical amount of freshwater is released, the meridional heat flux reduces abruptly to 0.2 PW ($1PW=10^{15}W/m^2$); this is particularly evident in the blow-up of the initiation phase given in Fig. 4. Deep water formation approaches very rapidly (within less than 100 years), and SST assumes interglacial values. The second, weaker melting peak is, in contrast to the previous one, associated with a continuous response of the thermohaline circulation. In Fig. 5 the overturning streamfunction in the Atlantic is shown at times a – f indicated in the time series of Figs. 3 and 4. At the height of the climatic event NADW formation has completely ceased to exist, and the deep water mainly consists of AABW. Obviously, the meridional heat transport recovers much faster (already at time d), because in the absence of an ice cover, the full flux boundary conditions determine the meridional heat flux. The deep circulation, on the other hand, recovers on a longer time scale. Note that only intermediate water is produced at time d in the Atlantic. At time f, convection has resumed down to the ocean bottom and the deep water masses show an essentially modern composition. This transient behaviour of the model is broadly consistent with the the oxygen isotope record from Greenland (Dansgaard *et al.*, 1989). Fast initiation, duration, rapid termination and a weaker, smooth cooling are modelled in good agreement with this paleoclimatic record.

These results are very encouraging, and our present efforts are directed towards a more realistic implementation of ice into the model.

4 Future Work

1. As is evident from the Appendix, surface exchange processes in the regions where deep water is formed need further attention. From the distribution of $\Delta^{14}C$ in the Southern Ocean we concluded that the residence time at the surface was either too long of gas exchange to fast. We will test whether the inclusion of marginal seas (Weddell Sea), increased meridional resolution

or finite zonal exchange time in the in the Southern Ocean are possible remedies. This will be the first point to be addressed as we wish to incorporate these results into an updated version of the Appendix that will be submitted to *Climate Dynamics* or *Paleoceanography* shortly.

2. Once we are confident that the surface exchange rates for different traces are consistent with those observed, a representation of the biological pump will be incorporated into the model in order to simulate more realistically the vertical gradients of total carbon and the pCO_2distribution at the ocean surface. This is achieved by including phosphate as an additional conserved tracer in the model. As a boundary condition we will restore surface values to the zonal averages of the observed phosphate (Levitus *et al.*, 1992). The model formulation will follow that of Najjar (1990). We will seek to incorporate a biological model that is simple enough so that is is consistent with the spatial and temporal resolution of the present model.

3. With the biological part included we will again assess the model performance to the present-day observations with particular attention to total carbon, alkalinity, phosphate and oxygen. To obtain optimal agreement the sensitivity to the few tunable parameters will be tested. Among these are the forcing salinities at the highest latitudes (see Appendix), gas exchange rates (with possible latitudinal dependence) and total inventories.

4. In collaboration with Dr. Daniel Wright, who is developing an ice model to be coupled to the present model, we will study the transient behaviour of the circulation when surface freshwater flux anomalies are applied. We can build on encouraging preliminary results reported in section 3 that may offer an explanation how the modern ocean circulation was established during the end of the last glacial. We will use the 1-layer ice model of Semtner (1976) with necessary adaptations for the present model. It is important, when doing integration over many thousands of years, that the salt and energy balances are exactly satisfied when sea ice cover is varying.

5. The transient runs shown in section 3 will be repeated with the inclusion of radiocarbon in the ocean and in a single, well-mixed atmospheric box. At steady state, a production rate of ^{14}C can be calculated which will be held constant. We will investigate how the

atmospheric inventory of ^{14}C will change during the dramatic transient evolution of the deep ocean circulation. This will help us in assessing how much of the variability of the atmsopheric radiocarbon concentration is due to circulation changes and whether it is, in principle, possible to generate the characteristic "plateaus" seen in the paleorecords.

6. The above transient runs will be repeated with the organic carbon cycle model included. Time series of the carbon and nutrient inventories will help to understand the dynamic behaviour of glacial-to-interglacial climate transitions.

References

Bojkov R.D., 1983, Report of the WMO (CAS) meeting of experts of the CO_2 concnetrations from pre-industrial times to IGY. *WCP-53, WMO, Geneva.*

Boyle E.A., L. Keigwin, 1987, North Atlantic thermohaline circulation during the past 20,000 years linked to high-latitude surface temperature. *Nature*, **330**, 35-40.

Broecker W.S., G.H. Denton, 1989, The role of ocean-atmosphere reorganisations in glacial cycles. *Geochim. Cosmochim. Acta*, **53**, 2465-2501.

Bryan F., 1986, High-latitude salinity effects and interhemispheric thermohaline circulations. *Nature*, **323**, 301-304.

Culkin F., 1965, The major constituents of sea water. In *Chemical Oceanography, Vol. 1*, J.P. Riley and G. Skirrow (eds.), Academic, p. 121-161.

Dansgaard W., J.W.C. White, S.J. Johnsen, 1989, The abrupt termination of the Younger Dryas climate event. *Nature*, **339**, 532-534.

Duplessy J.C., N.J. Shackleton, R.G. Fairbanks, L. Labeyrie, D. Oppo, N. Kallel, 1989, Deepwater

source variations during the last climatic cycle and their impact on the global deepwater circulation. *Paleoceanogr.*, **3**, 343-360.

Fairbanks R.G., 1989, A 17,000-year glacio-eustatic sea level record: influence of glacial melting rates on the Younger Dryas event and deep-ocean circulation. *Nature*, **342**, 637-642.

Levitus S., 1982, Climatological Atlas of the World Ocean. *NOAA Prof. Paper*, **13**, 177p.

Levitus S., J.L. Reid, M.E. Conkright, R. Najjar, 1992, Distribution of nitrate, phosphate and silicate in the world oceans. *Progr. Oceanogr.*, (submitted).

Maier-Reimer E., K. Hasselmann, 1987, Transport and stroage of CO_2 in the ocean – an inorganic ocean-circulation carbon cycle model. *Climate Dyn.*, **2**, 63-90.

Maier-Reimer E., U. Mikolajewicz, 1989, Experiments with an OCGM on the cause of the Younger Dryas. *Max Planck Institut für Meteorologie, Hamburg, Germany*, **39**, 13p.

Manabe S., R.J. Stouffer, 1988, Two stable equilibria of a coupled ocean-atmosphere model. *J. Climate*, **1**, 841-866.

Marotzke J., J. Willebrand, 1991, Multiple equilibria of the global thermohaline circulation. *J. Phys. Oceanogr.*, **21**, 1372-1385.

Mehrbach C., C.H. Culberson, J.E. Hawley, R.M. Pytkowicz, 1973, Measurement of the apparent dissociation constants of carbonic acid in seawater at atmospheric pressure. *Limnology and Oceanogr.*, **18**, 897-907.

Najjar R.G, 1990, Simulations of the phosphorus and oxygen cycles in the world ocean using a general circulation model. *Ph.D. thesis Princeton University*, 190p.

Rotty R.M., 1981, Data for global CO_2 production from fossil fuel and cement. In *Carbon Cycle Modelling*, B. Bolin (ed.), Wiley, 121-125.

Sarmiento J.L., J.C. Orr, U. Siegenthaler, 1992, A perturbation simulation of CO_2 uptake in an ocean general circulation model. *J. Geophys. Res.*, (in press).

Semtner A.J. 1976, A model for the thermodynamic growth of sea ice in numerical investigations of climate. *J. Phys. Oceanogr.*, **6**, 379-389.

Siegenthaler U., H. Oeschger, 1987, Biospheric CO_2 emissions during the past 200 years reconstructed by deconvolutions of ice core data. *Tellus*, **39B**, 140-154.

Stocker T.F., D.G. Wright, 1991a, Rapid transitions of the ocean's deep circulation induced by changes in surface water fluxes. *Nature*, **351**, 729-732.

Stocker T.F., D.G. Wright, 1991b, A zonally averaged ocean model for the thermohaline circulation. Part II: Interocean circulation in the Pacific-Atlantic basin system. *J. Phys. Oceanogr.*, **21**, 1725-1739.

Stocker T.F., D.G. Wright, L.A. Mysak, 1992a, A zonally averaged, coupled ocean-atmosphere model for paleoclimatic studies. *J. Climate*, (in press).

Stocker T.F., D.G. Wright, W.S. Broecker, 1992b, The influence of high-latitude surface forcing on the global thermohaline circulation, (in preparation).

Sundquist, E.T., 1985, Geological perspectives on carbon dioxide and the carbon cycle. In *The Carbon Cycle and Atmospheric CO_2: Natural Variations Archean to Present*, E.T. Sundquist and W.S. Broecker (eds.), Geophys. Monograph., **32**, American Geophysical Union, 5-59.

Takahashi T., W.S. Broecker, A.E. Bainbridge, R.F. Weiss, 1980, Carbonate chemistry of the Atlantic, Pacific and Indian Oceans: The results of the GEOSECS expeditions, 1972-1978. *Lamont-Doherty Geological Observatory, Tech. Rep.*, **CV-1-80**, 196p.

Takahashi T., W.S. Broecker, A.E. Bainbridge, 1981, The alkalinity and total carbon dioxide in the world oceans. In *Carbon Cycle Modelling*, B. Bolin (ed.), Wiley, 271-286.

Weiss R.F., 1974 Carbon dioxide in water and seawater: the solubility of a non-ideal gas. *Mar. Chem.*, **2**, 203-215.

Welander P., 1986, Thermohaline Effects in the ocean circulation and related simple models. In *Large-Scale Transport Processes in the Ocean and Atmosphere*, J. Willebrand and D.L.T.

Anderson (eds.), Reidel, 163-200.

Wright D.G., T.F. Stocker, 1991, A zonally averaged ocean model for the thermohaline circulation. Part I: Model development and flow dynamics. *J. Phys. Oceanogr.*, **21**, 1713-1724.

Wright D.G., T.F. Stocker, 1992, Sensitivities of a zonally averaged global ocean circulation model. *J. Geophys. Res.*, (submitted)

Zhang S., R.J. Greatbatch, C.A. Lin, 1992, A re-examination of the polar halocline catastrophe and implications for coupled ocean-atmosphere modelling. *J. Phys. Oceanogr.*, (submitted).

Tables

	This Model	Hamburg	Princeton	Observations
ΣC(ocean)	38979 Gt	?	[perturbation model]	36600 - 38400 Gt
$p\mathrm{CO}_2$ (1800 AD)	280.8 ppm	290 ppm	280.0 ppm	281±7 ppm
ΣC(atmosphere)	604.8 Gt	615 Gt	?	550 - 590 Gt
A_0	0.149	0.142	0.174	-
A_1, τ_1 [years]	0.208, 303.7	0.241, 313.8	0.275, 376.6	-
A_2, τ_2 [years]	0.327, 88.2	0.323, 79.8	0.307, 67.7	-
A_3, τ_3 [years]	0.178, 21.2	0.206, 18.8	0.189, 10.7	-
A_4, τ_4 [years]	0.139, 3.1	0.088, 1.7	0.054, 0.9	-

Table 1: Comparison of some model characteristics with the Hamburg model (Maier-Reimer & Hasselmann, 1987), the Princeton model (Sarmiento , 1992) and observations (Sundquist, 1985; Siegenthaler & Oeschger, 1987)

Figure Captions

Figure 1: Difference of oceanic and atmospheric pCO_2 for a typical steady state in the three ocean basin. Note that the latitudinal gradients are large because the biological pump is not yet included in the model.

Figure 2a: Evolution of the airborne fraction $a(t)$ for a $2\times CO_2$ experiment. The present model results (solid) are very close to those of the Hamburg model (1-dashed, Maier-Reimer & Hasselmann, 1987), while the Princeton model (2-dashed, Sarmiento *et al.*; 1992) exhibits lower oceanic uptake rates.

Figure 2b: Input of anthropogenic carbon into the atmosphere according to Rotty (I-solid, 1981), biogenic input estimate of Bojkov (B-solid, 1983) and reconstructed input (R-solid) required by the model when forced with the Rotty-input.

Figure 3: Time series of some model characteristics through the Fairbanks (1989) melting history. The evolution of the net freshwater flux into the ocean at 14°N is given in (a). Note that the steady state at this latitude shows evaporation of about 0.1Sv. During the first and stronger melt water peak, (a), sea surface temperature in the northern North Atlantic (at 72°N) drops to freezing temperature, (b), caused by an interruption of NADW formation, (c), and reduction of the associated meridional heat flux, (d). After the peak the conveyor belt recovers in less than 100 years. The second, smaller melting event causes only a relatively weak cooling. Six times (a)–(f) are indicated for which the Atlantic overturning streamfunction is given in Figs. 5a – 5f.

Figure 4: Blow up of the initiation time of the melting event. While sea surface temperature drops smoothly, (a), NADW formation, (b), and the meridional heat flux, (c), shut off abruptly after a continuous reduction down to a critical value.

Figure 5: Overturning streamfunction in the North Atlantic during the times (a)–(f) indicated in Figs. 3 and 4.

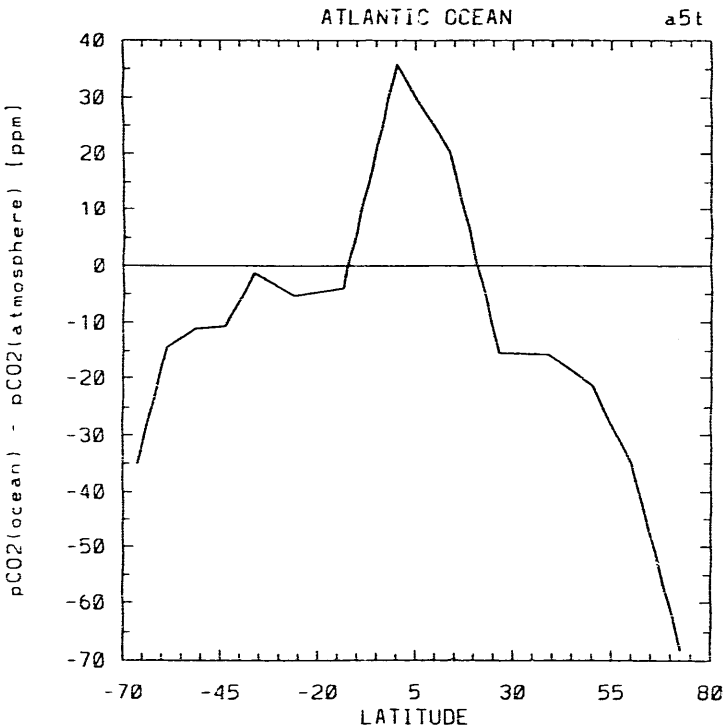
ATLANTIC OCEAN
a5t
pCO2(ocean) - pCO2(atmosphere) [ppm]
40
30
20
10
0
-10
-20
-30
-40
-50
-60
-70
-70
-45
-20
5
30
55
80
LATITUDE

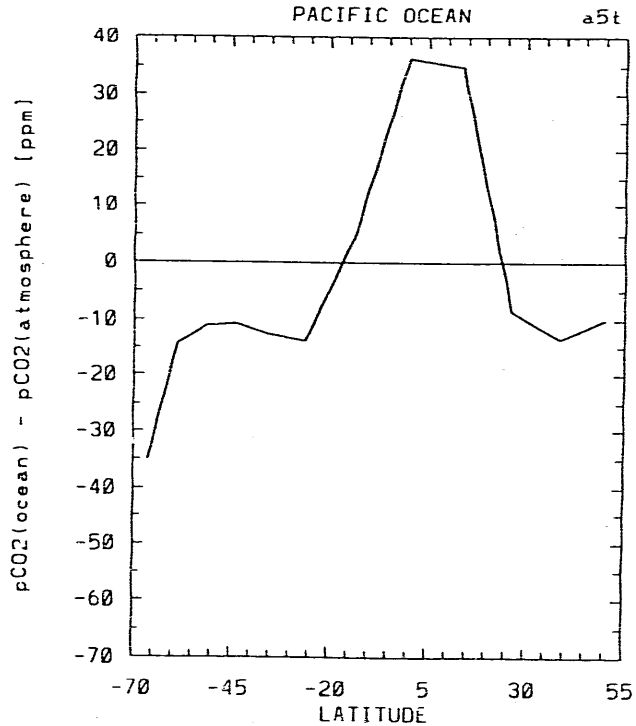
PACIFIC OCEAN
a5t
pCO2(ocean) - pCO2(atmosphere) [ppm]
40
30
20
10
0
-10
-20
-30
-40
-50
-60
-70
-70
-45
-20
5
30
55
LATITUDE

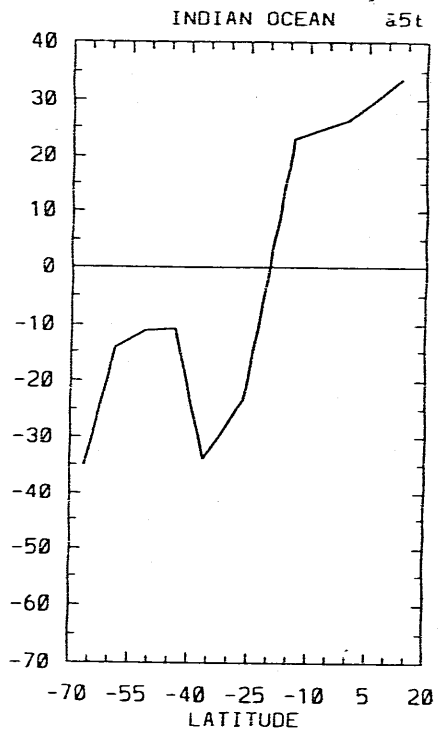
INDIAN OCEAN
a5t
40
30
20
10
0
-10
-20
-30
-40
-50
-60
-70
-70
-55
-40
-25
-10
5
20
LATITUDE

Fig 1

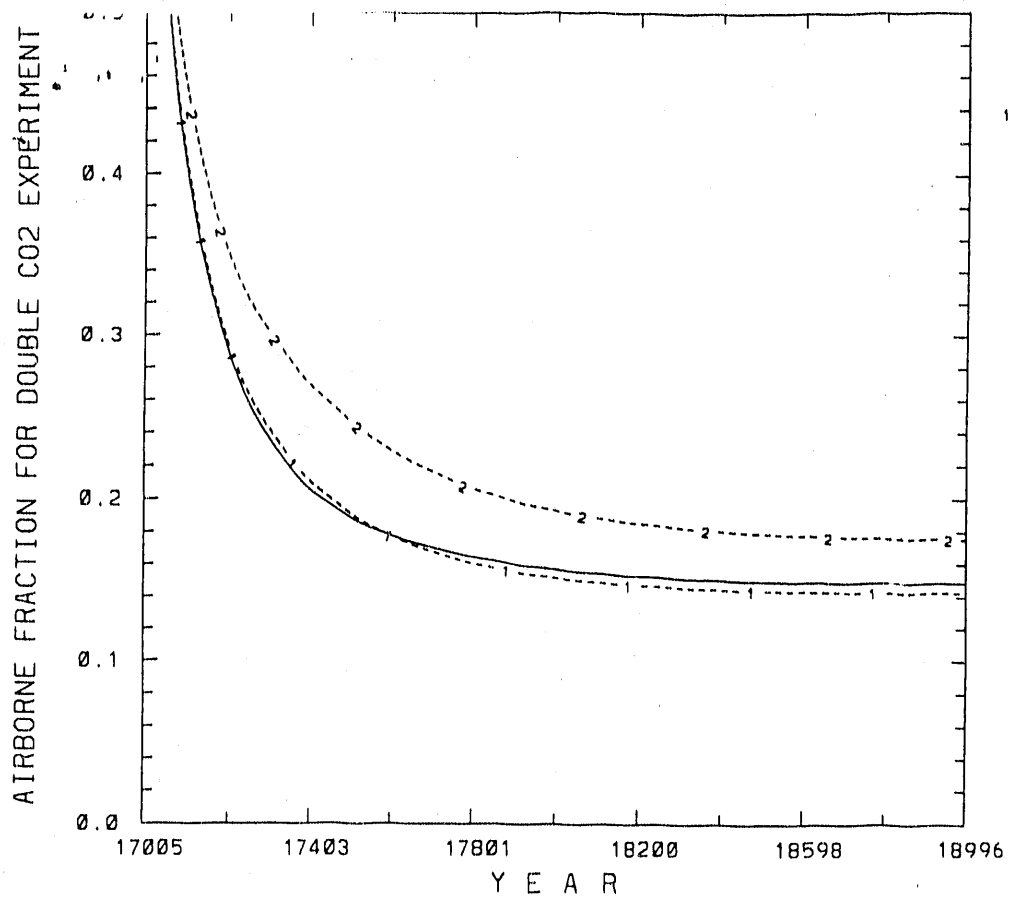
AIRBORNE FRACTION FOR DOUBLE CO2 EXPERIMENT
0.0
0.1
0.2
0.3
0.4
17005
17403
17801
18200
18598
18996
Y E A R

Fig 2a

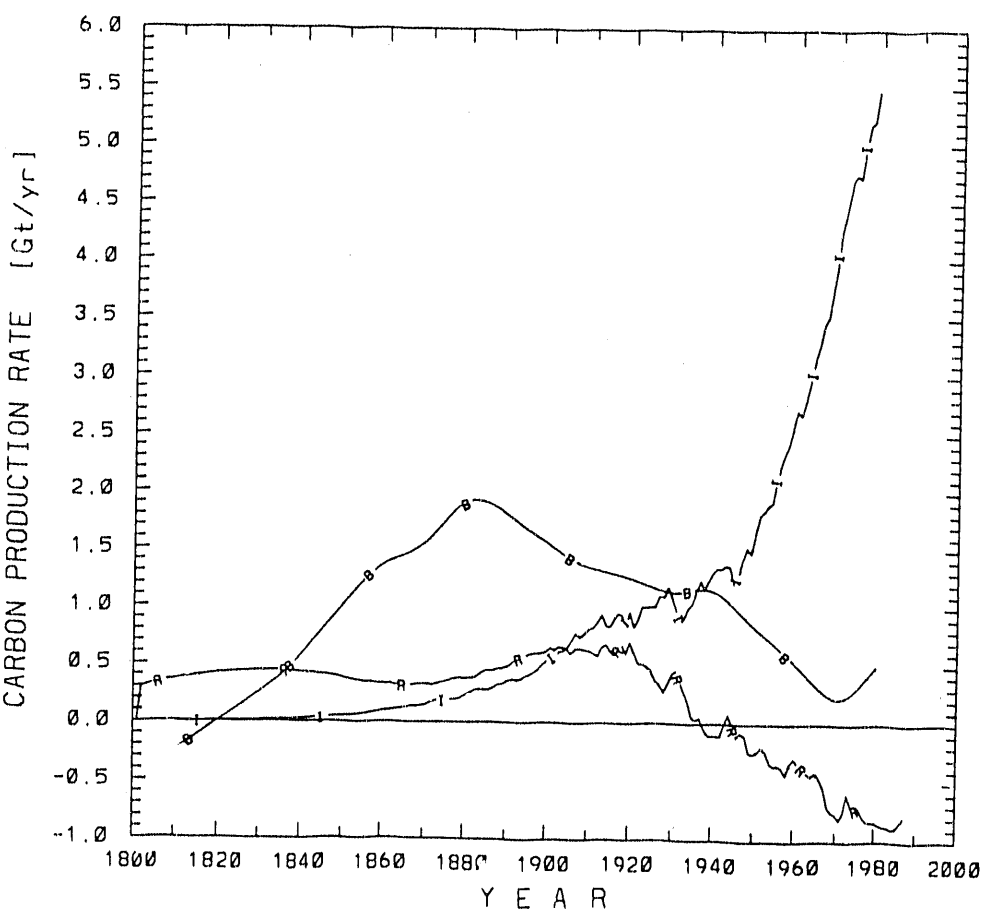
CARBON PRODUCTION RATE [Gt/yr]
6.0
5.5
5.0
4.5
4.0
3.5
3.0
2.5
2.0
1.5
1.0
0.5
0.0
-0.5
-1.0
1800
1820
1840
1860
1880
1900
1920
1940
1960
1980
2000
Y E A R

Fig 2b

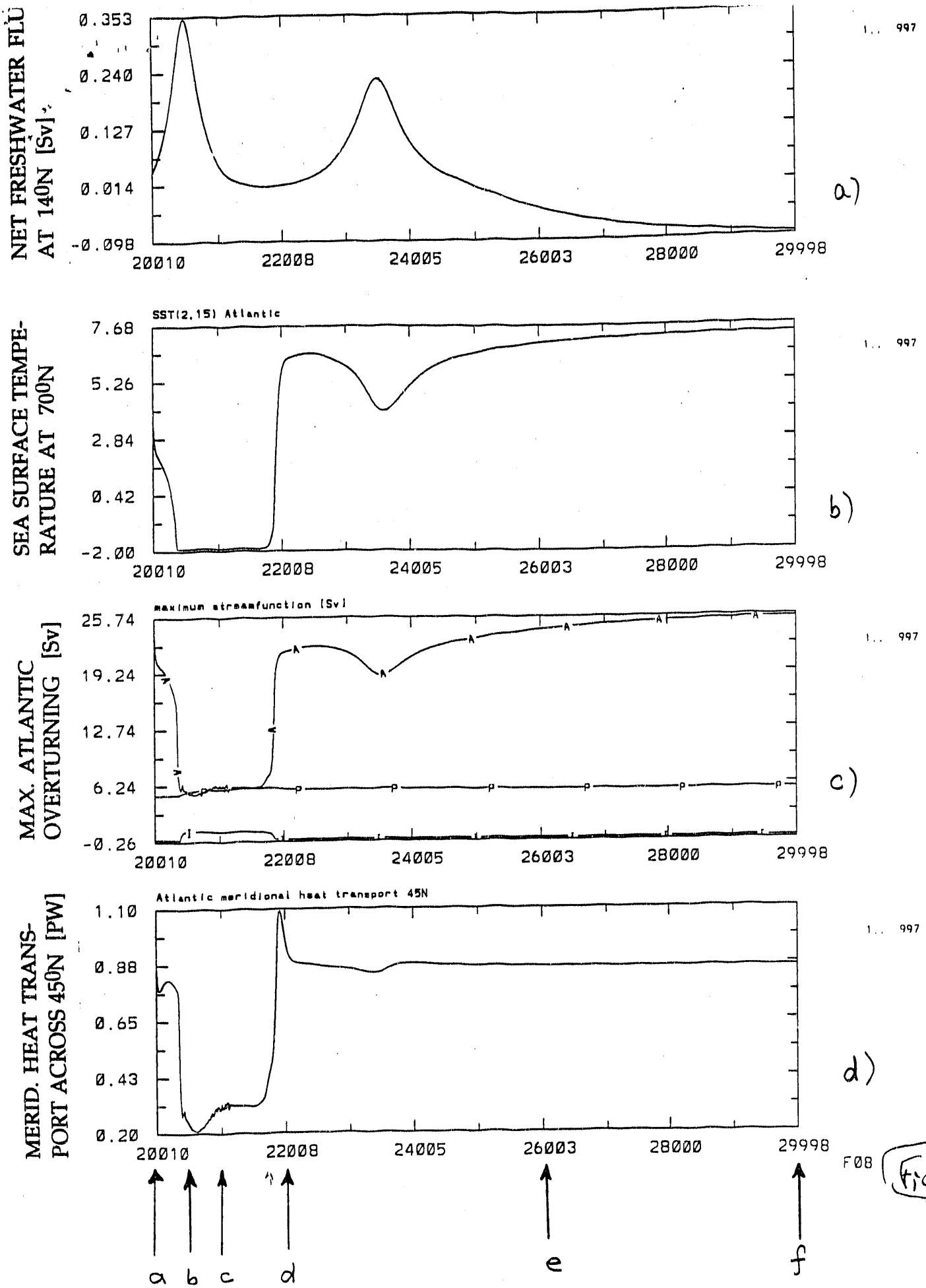
NET FRESHWATER FLU
AT 140N [Sv]
0.353
0.240
0.127
0.014
-0.098
20010
22008
24005
26003
28000
29998
a)
SST(2,15) Atlantic
SEA SURFACE TEMPE-
RATURE AT 70ºN
7.68
5.26
2.84
0.42
-2.00
b)
maximum streamfunction [Sv]
MAX. ATLANTIC
OVERTURNING [Sv]
25.74
19.24
12.74
6.24
-0.26
c)
Atlantic meridional heat transport 45N
MERID. HEAT TRANS-
PORT ACROSS 45ºN [PW]
1.10
0.88
0.65
0.43
0.20
d)
a
b
c
d
e
f

F08 Fig 3

BLOW-UP OF INITIATION PHASE

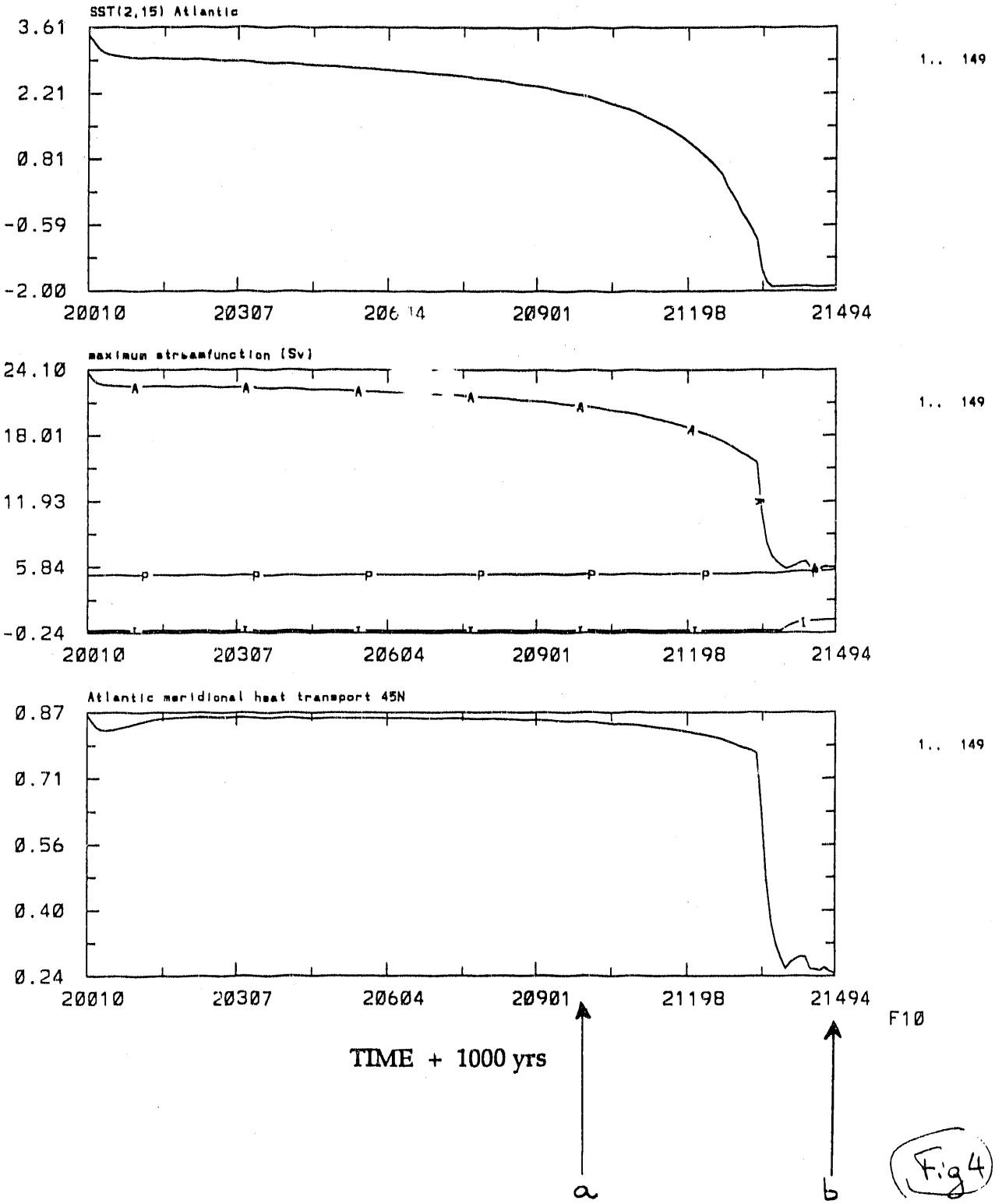

Fig 4

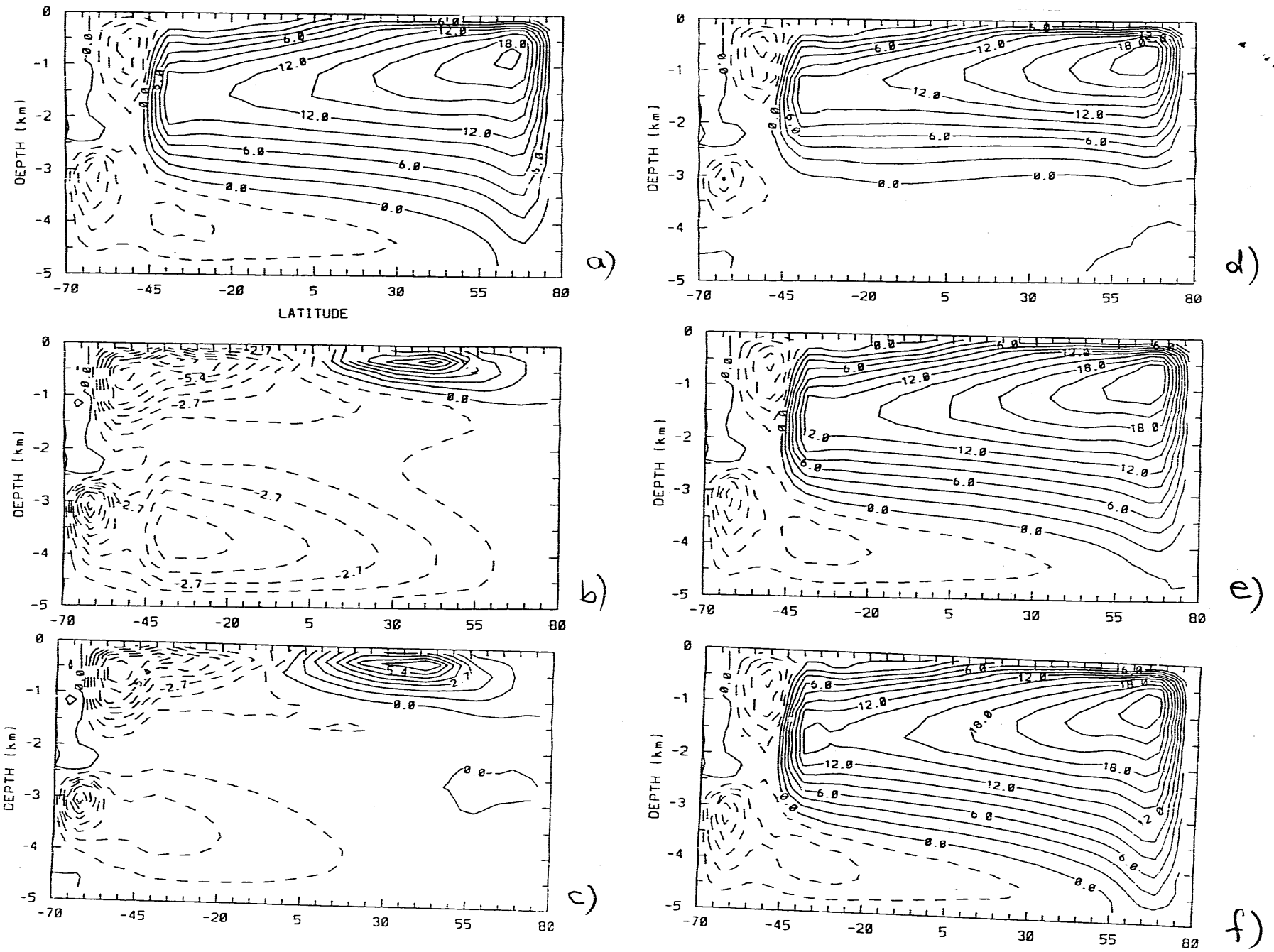
ATLANTIC STREAMFUNCTION [Sv]
DEPTH (km)
LATITUDE
-70
-45
-20
5
30
55
80
0
-1
-2
-3
-4
-5
a)
b)
c)
d)
e)
f)

Fig. 5

END

DATE
FILMED
6/15/92